



ELSEVIER

Available online at [www.sciencedirect.com](http://www.sciencedirect.com)

SCIENCE @ DIRECT®

Journal of Sound and Vibration 282 (2005) 411–427

JOURNAL OF  
SOUND AND  
VIBRATION

[www.elsevier.com/locate/jsvi](http://www.elsevier.com/locate/jsvi)

# Drop-weight test based identification of elastic half-space model parameters

P. Ruta\*, A. Szydło

*Institute of Civil Engineering, Wrocław University of Technology, Wyb. Wyspińskiego 27, 50–370 Wrocław, Poland*

Received 26 March 2003; accepted 25 February 2004

---

## Abstract

A method enabling the conversion of dynamic drop-weight test results into a statical substitute is presented. Owing to this substitution, statical models, instead of complex dynamical models, can be used for subsoil elastic moduli identification. An elastic half-space was adopted as the subsoil model. Identification was limited to the determination of the subsoil's modulus of elasticity.

The results were verified in two ways. One way consisted in the simulation of experimental results on the basis of theoretical results. The latter were obtained by analytically solving the problem of half-space vibrations caused by an impact pulse. The elastic moduli identified on the basis of the simulated results were compared with the assumed elastic moduli. In the other verification method, the results obtained by the proposed identification method were compared with the result yielded by the standard statical identification method. The load and displacement values used were from tests carried out on actual soils.

© 2004 Elsevier Ltd. All rights reserved.

---

## 1. Introduction

In the case of engineering structures which interact with the ground base, such as road and airfield pavements and track structures, it is essential to know the ground base model parameters. The most common ground base model is an elastic half-space described by a modulus of elasticity ( $E$ ) and the Poisson ratio ( $\nu$ ). Methods of determining ground base moduli can be classified into

---

\*Corresponding author.

*E-mail address:* [piotr.ruta@pwr.wroc.pl](mailto:piotr.ruta@pwr.wroc.pl) (P. Ruta).

two groups: laboratory methods and in situ (field) methods. In a laboratory, the moduli are determined from: triaxial tests, consolidometer tests or the correlation with the ground's bearing capacity index—the California Bearing Ratio (CBR) [1]. In in situ investigations the moduli are determined by tests consisting in loading the ground base with a pressure plate. Depending on how the plate is loaded, the methods of estimating ground base moduli can be divided into [2–4]:

- static methods—a load is statically applied to the pressure plate and the displacements of the latter are measured,
- impact methods—a load is applied in an impactive manner (an impulse is produced by a dropped weight) and the displacements of the pressure plate are measured,
- vibrational methods—vibrations having different frequencies are produced in the ground base and the wave propagation velocities are measured.

The identification of the moduli in in situ investigations consists in backcalculation, i.e. the moduli are determined for known pressure plate displacements under a static load or an impact load or for a known wave propagation velocity (vibrational methods).

In the construction of roads and airports, static and impact methods are most commonly used. Drop-weight tests are less time-consuming than static load tests. A drop-weight test at one measuring position takes about 2–3 min to perform whereas a static load test takes 1–2 h. The moduli are calculated from the following relations [1,4,5]:

$$E_s = \frac{2(1 - \nu^2)Q_s}{\pi a q_{s \max}}, \quad E_d = \frac{2(1 - \nu^2)Q_{\max}}{\pi a q_{0 \max}}, \quad (1,2)$$

where  $E_s$  is a static modulus,  $E_d$  the dynamic modulus (determined from drop-weight test results),  $Q_s$  the maximum static load,  $Q_{\max}$  the maximum dynamic load,  $a$  the pressure plate's radius,  $q_{s \max}$  the maximum plate displacement under the static load,  $q_{0 \max}$  the maximum plate displacement under the impact load and  $\nu$  the Poisson ratio assumed to be known.

For the same ground base, the same load values ( $Q_s = Q_{\max}$ ), the same pressure plate radii  $a$  and the same Poisson ratios, different values of moduli  $E_s$  and  $E_d$  are obtained. This is due to the fact that different plate displacement values are registered for static loads  $q_{s \max}$  and dynamic loads  $q_{0 \max}$ . Therefore coefficients  $f$  of the correlation between the identified moduli  $E_s = fE_d$  are sought. According to Refs. [1,5], correlation coefficient  $f$  is in interval  $\langle 2,5 \rangle$ .

In this paper, a method of converting drop-weight test results into static load test results, based on the previous research findings [6], is described and verified. The method makes it possible to use static models instead of complicated dynamic models in the process of identification. An elastic half-space was used as the base ground model. Assuming the Poissons' coefficient values to be known, identification was limited to moduli of elasticity.

The method was verified in two ways. First, by simulating experimental results with theoretical results. The latter were obtained by analytically solving the problem of elastic half-space vibrations (produced by a hypothetical impact) for a priori known values of elasticity moduli (see Appendix B). The identified values were compared with the a priori assumed values of the moduli. The other way consisted in the use of experimental in situ investigations carried out by the authors. The moduli were determined by the static method and the impact method. In the latter case, the proposed method of identifying the moduli of elasticity was used and the identified moduli were compared with the ones obtained from the static load tests.

## 2. Problem formulation

The identification of the moduli of an elastic ground base model on the basis of drop-weight test results is considered. The test is performed using a drop-weight tester—a mechanical device which delivers a controlled impulse of a finite intensity and duration to a horizontal surface structure. A pictorial diagram of the drop-weight tester and its simplified model are shown in Figs. 1 and 2. The drop-weight tester consists of movable mass  $m$ , a shock absorber in the form of an elastodamping constraint with parameters  $k$ ,  $c$  and a pressure plate which transfers the shock absorber's reaction to the structure. The drop-weight tester operates like this: mass  $m$  free falling from height  $h_0$  delivers an impact and deadweight load  $G = mg$  to the shock absorber which undergoes deformation and transmits force  $Q(t)$  to the structure. At instant  $t_1$  during inverse motion the mass separates from the shock absorber and lifts to height  $h_1$ . The shock absorber's function is to reduce the impact and transform it into an impulse with finite parameters.

Dynamic load  $Q(t)$  (more precisely, total impulse  $\int Q(t) dt$ ) and displacement  $q_0(t)$  of the central point (under the pressure plate's centre) of the system's boundary surface are the basis for the identification of the sought ground base moduli. Because of the limitation of the measurements to one point (dictated by the device's measuring capabilities) only ground base models with one deformation parameter unknown are considered. Hence a homogenous, isotropic, elastic half-space with the known Poisson ratio was adopted as the ground base model in this paper. The identified modulus of elasticity of the ground base is a certain “substitute” model which globally characterizes the heterogeneous ground base. Therefore it should not be identified with the moduli determined by tests performed on ground base samples.

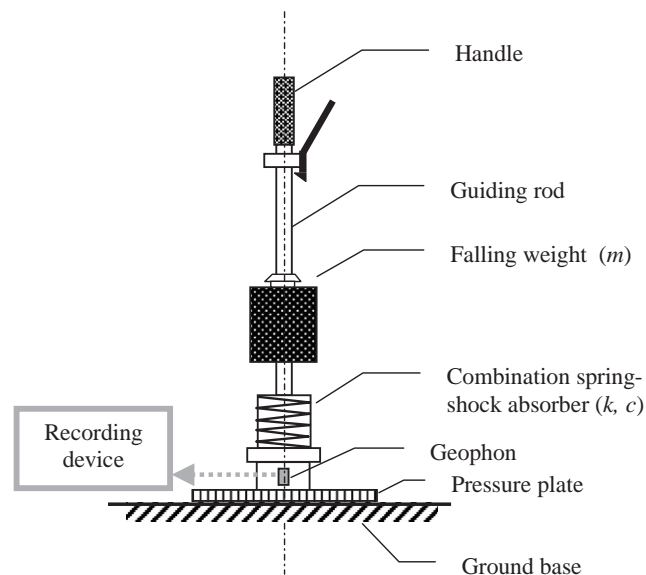


Fig. 1. Schematic diagram of drop-weight tester.

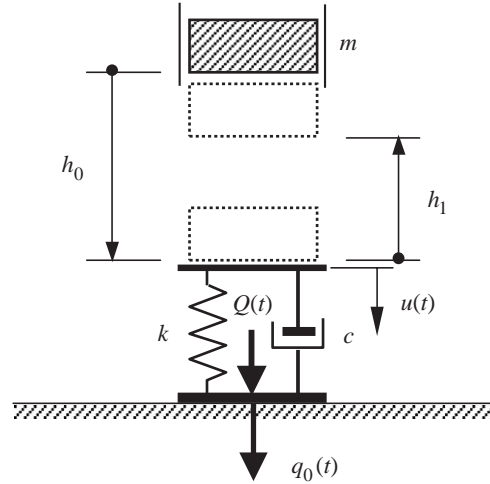


Fig. 2. Model of drop-weight tester.

### 3. Drop-weight test as substitute for static load test [6]

The produced (by the drop-weight tester) impulse  $p(r, t) = \phi(r)Q(t)$ , distributed within a circular area with radius  $a$ , impinging on the boundary surface generates a displacement field in the ground base. Impulse spatial distribution function  $\phi(r)$  is assumed to be so normalized that  $2\pi \int_0^a \phi(r)r dr = 1$ . Then function  $Q(t)$  represents the resultant of the impinging load. Resultant  $Q(t)$  is realized in finite time, its course is arbitrary but total time effect  $\hat{Q}_s = \int_0^\infty Q(t) dt \neq 0$  and is limited  $|\hat{Q}_s| < \infty$ . It is also assumed that the vertical displacement of the boundary surface at point “ $i$ ”, denoted by  $q_i(t)$ , is measured in the drop-weight test.

As it is proven in Appendix A, if system displacement  $q_i(t)$  caused by load  $Q(t)$  is known, then without performing any additional tests one can determine system displacement  $\hat{q}_i(t)$  caused by load  $\hat{Q}(t) = \int_0^t Q(t) dt$ . In this case, the displacement has the following form:  $\hat{q}_i(t) = \int_0^t q_i(t) dt$ . Illustrative graphs of functions  $Q(t)$ ,  $q_i(t)$  and  $\hat{Q}(t)$ ,  $\hat{q}_i(t)$  are shown in Fig. 3. It is apparent that for the assumptions made load  $\hat{Q}(t)$  at  $t \rightarrow \infty$  approaches a constant:

$$\lim_{T \rightarrow \infty} \hat{Q}(T) = \lim_{T \rightarrow \infty} \int_0^T Q(t) dt = \int_0^\infty Q(t) dt = \hat{Q}_s = \text{const.} \quad (3)$$

At the same time it is known that if a signal approaching a constant is introduced at an actual system’s input, owing to damping also the system response will approach a constant equal to the static response:

$$\lim_{t \rightarrow \infty} \hat{q}_i(t) = \lim_{t \rightarrow \infty} \int_0^t q_i(t) dt = \int_0^\infty q_i(t) dt = \hat{q}_{is} = \text{const.} \quad (4)$$

Thus, by measuring functions  $Q(t)$ ,  $q_i(t)$  one can determine system static flexibility  $\delta_i = \hat{q}_{is} / \hat{Q}_s$  (i.e. the static displacements of point “ $i$ ”, corresponding to load  $\hat{Q}_s = 1$ ). The flexibility is expressed by

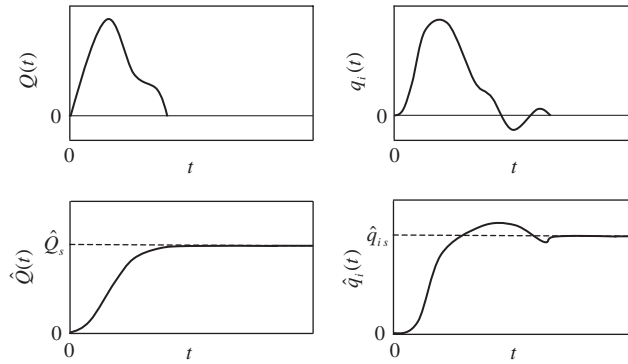


Fig. 3. Illustrative graphs of functions  $Q(t)$ ,  $q_i(t)$ ,  $\hat{Q}(t)$ ,  $\hat{q}_i(t)$ .

this formula

$$\delta_i = \frac{\int_0^\infty q_i(t) dt}{\int_0^\infty Q(t) dt}. \tag{5}$$

Formula (5) relates the results of an actual dynamic test and those of the corresponding hypothetical static load test. Thus, the conditions for substituting a dynamic test for a static test have been defined. Formula (5) also applies to linear viscoelastic rheological solid bodies if  $\delta_i$  is understood as static flexibility in the boundary sense ( $t \rightarrow \infty$ ).

#### 4. Identification of elastic ground base model’s moduli of elasticity

The relations presented above were used to identify the elastic ground base model’s parameters. In this process, the ground base is subjected to a dynamic impact test. The obtained measurements, i.e. the trace of impulse  $Q(t)$  and displacement  $q_0(t)$  of the ground base boundary surface’s central point (under the plate’s centre) caused by this impulse form the basis for determining the model’s deformation parameters.

A homogenous, isotropic, elastic half-space was adopted as the ground base model, assuming that the Poisson ratio for the half-space is known. The vertical displacements of half-space boundary surface  $z = 0$ , assuming that the spatial distribution of the load is constant

$$\phi(r) = \begin{cases} P/\pi a^2 & \text{for } r \leq a, \\ 0 & \text{for } r > a \end{cases} \tag{6}$$

is described by this equation

$$q(r) = \begin{cases} \frac{4(1-\nu^2)P}{\pi^2 a E} E\left(\frac{r}{a}\right) & \text{for } r \leq a, \\ \frac{4(1-\nu^2)Pr}{\pi^2 a^2 E} \left( E\left(\frac{a}{r}\right) - \left(1 - \frac{a^2}{r^2}\right) K\left(\frac{a}{r}\right) \right) & \text{for } r > a, \end{cases} \tag{7}$$

where  $E$  is the modulus of elasticity (Young’s modulus) of the half-space and  $E(k)$ ,  $K(k)$  are the full elliptic integrals. The assumption that the distribution is uniform is based on research on load distributions under plates [4,7].

The static flexibility of the ground base model at point  $r = 0$ , determined from (7), is expressed by this formula

$$\delta_0 = \frac{w(0)}{P} = \frac{2(1 - \nu^2)}{\pi a E}, \quad (8)$$

whereas the static flexibility determined from dynamic impact test results is given by formula (5). After the right sides of Eqs. (5) and (8) are compared the formula for the sought modulus of elasticity of the ground base assumes this final form

$$E = \frac{2(1 - \nu^2)}{\pi a} \frac{\int_0^\infty Q(t) dt}{\int_0^\infty q_0(t) dt}. \quad (9)$$

Since not all the testers known to the authors can register the trace of load function  $Q(t)$ , integral  $\int_0^\infty Q(t) dt$  which occurs in formulas (5) and (9) can be determined on the basis of the height from which movable mass  $m$  falls and the height to which it subsequently rebounds (see Fig. 2). The heights are denoted as  $h_0$  and  $h_1$ , respectively. Force  $Q(t)$  is generated during the contact of the moving mass with the shock absorber, i.e. in time interval  $\langle 0, t_1 \rangle$ . The value of the force is

$$Q(t) = G - m\ddot{u}, \quad (10)$$

and the complete impulse amounts to

$$\hat{Q}_s = \int_0^\infty Q(t) dt = \int_0^{t_1} Q(t) dt = Gt_1 - m\dot{u}(t_1) + m\dot{u}(0). \quad (11)$$

The initial velocity is  $\dot{u}(0) = \sqrt{2gh_0}$  and the fact that the mass rebounds to height  $h_1$  indicates that  $\dot{u}(t_1) = -\sqrt{2gh_1}$ . Formula (11) can be written as

$$\hat{Q}_s = m(\sqrt{2gh_0} + \sqrt{2gh_1}) + Gt_1. \quad (12)$$

## 5. Theoretical simulation of drop-weight test

To verify the method described in Section 3 and to demonstrate its effectiveness a simulation of the drop-weight test was run. The simulation consists in replacing measurements with the results obtained from analyses made for an assumed, known ground base model (see Appendix B). Also the function which describes the impactor impingement on the ground base was determined analytically, assuming that it is expressed by this formula

$$Q(t) = \begin{cases} Q_{\max} \sin(\pi t/t_1) & \text{for } 0 \leq t \leq t_1, \\ 0 & \text{for } t > t_1. \end{cases} \quad (13)$$

The interaction between the half-space and the drop-weight tester's pressure plate was assumed to be uniformly distributed.

Let us assume that the following ground base parameters are known: modulus of elasticity  $E$ , the Poisson ratio  $\nu$  and density  $\rho$ . Using the above form of function  $Q(t)$  one can determine ground base vertical displacement function  $q_0(t)$  at point  $(r, z) = (0, 0)$  (see Appendix B). The theoretically determined displacements are regarded as experimental displacements. Elasticity modulus values:  $E = 5, 25, 50, 100, 200$  MPa were assumed for the computations. The other parameters were:  $\nu =$

0.3,  $\rho = 2000 \text{ kg/m}^3$ . Also impulse duration  $t_1$  was varied. The computations were performed for the following impulse durations  $t_1 = 2.5, 5, 10, 15, 20$  ms. The maximum impulse was  $Q_{\max} = 7.0 \text{ kN}$ .

The obtained results were identified using the procedure described in Section 3. Applying formula (9) elasticity modulus  $\check{E}$  was calculated. The assumed values of  $E$  and the identified values of  $\check{E}$  are shown in Table 1 which also shows modulus of elasticity  $\check{E}$  calculated from this formula

$$\check{E} = \frac{2(1 - \nu^2)}{\pi a} \frac{Q_{\max}}{q_{0 \max}}, \quad (14)$$

where  $Q_{\max}$  and  $q_{0 \max}$  are the maximum values of, respectively, dynamic impact load  $Q(t)$  and displacement  $q_0(t)$  caused by the load. The formula is based on the assumption that static flexibility can be expressed as follows

$$\delta_0 = \frac{q_{0 \max}}{Q_{\max}}. \quad (15)$$

Formula (15) is commonly used by manufacturers of drop-weight testers for determining the static flexibilities of ground base systems. Regrettably, in the drop-weight tester documentation available to the authors no theoretical or experimental validation of the formula is given.

The analysis shows that for short impulses (2.5, 5 ms) the errors in the identification of elasticity moduli by formula (14) range from 1.1% to 176.6% (the shorter the impulse, the larger the identification error). For longer impulses (10, 15, 20 ms) the identification error decreases to 0.01–12.0%. It becomes apparent that the identification error in the case of formula (14) also depends on the value of modulus  $E$ : the error is the larger, the lower the value of  $E$ . A closer analysis shows that the error is the larger, the lower is the ratio of impulse duration to the time which the Rayleigh wave needs to travel distance  $a$  (see the last column in Table 1). Unlike formula (14), the proposed identification method based on the substitution of drop-weight test results for static load test results (formula (9) is used to determine the modulus of elasticity of the ground base) does not introduce such errors: the maximum simulation test error is below 0.0002% and it is due to numerical errors (not to the identification method). The normalized diagrams of displacements  $q_0(t)E_i$  caused by an impulse of  $t_1 = 5$  ms duration for elasticity moduli  $E_1 = 5 \text{ MPa}$ ,  $E_2 = 25 \text{ MPa}$ ,  $E_3 = 200 \text{ MPa}$  and their quasi-static background (the solution of the problem with neglected ground base inertial forces) are shown by the dotted line in Fig. 4.

## 6. Identification of ground base moduli by in situ drop-weight test method

The proposed method of replacing static load test results with equivalent drop-weight test results was used to identify moduli of elasticity in situ. The identification tests were performed using a light ZFG 02 dynamic deflectometer [5]. This device produces a maximum impact of 7.07 kN which for the plate diameter of 30 cm gives a base compression of 0.1 MPa. The impulse duration is 18 ms. Three kinds of ground base:

- clay soil with a consolidation index of 0.99;
- sandy soil with three different consolidation indices: 0.98, 0.94, 0.90;
- a 10 cm thick layer of soil stabilized with cement, laid on sandy soil with a consolidation index of 0.98

Table 1  
Results of simulation test

$t_1$ (ms)	$E$ (MPa)	$\hat{Q}_s$ (N s)	$\hat{q}_{0,s}$ ( $10^{-6}$ ms)	$\tilde{E}$ (MPa)	Error $\frac{E-\tilde{E}}{E}$ 100%	$Q_{\max}$ (N)	$q_{0\max}$ ( $10^{-4}$ m)	$\tilde{E}$ (MPa)	Error $\frac{E-\tilde{E}}{E}$ 100%	$t_1/(ax_3/c_2)$
2.5	5	11.14	8.606	5.000	0	7000	19.54	13.83	176.6	0.48
	25		1.721	25.00	0		7.540	35.86	43.4	1.07
	50		0.8606	50.00	0		4.505	60.01	20.0	1.52
	100		0.4303	100.0	0		2.471	109.4	9.4	2.14
	200		0.2151	200.0	0		1.293	209.1	4.6	3.03
5	5	22.28	17.21	5.000	0	7000	35.31	7.655	53.3	0.96
	25		3.442	25.00	0		9.883	27.35	9.4	2.14
	50		1.721	50.00	0		5.171	52.29	4.6	3.03
	100		0.8606	100.0	0		2.643	102.2	2.2	4.29
	200		0.4303	200.0	0		1.337	202.2	1.1	6.06
10	5	44.56	34.42	5.000	0	7000	48.30	5.598	12.0	1.92
	25		6.884	25.00	0		10.58	25.56	2.2	4.29
	50		3.442	50.00	0		5.347	50.56	1.1	6.06
	100		1.721	100.0	0		2.689	100.6	0.6	8.57
	200		0.8606	200.0	0		1.348	200.6	0.3	12.13
15	5	66.85	51.63	5.000	0	7000	51.45	5.255	5.1	2.86
	25		10.33	25.00	0		10.71	25.25	1.0	6.43
	50		5.163	50.00	0		5.380	50.25	0.5	9.09
	100		2.582	100.0	0		2.697	100.2	0.2	12.86
	200		1.291	200.0	0		1.350	200.2	0.1	18.19
20	5	89.13	68.85	5.000	0	7000	52.58	5.141	2.8	3.83
	25		13.77	25.00	0		10.75	25.14	0.6	8.57
	50		6.884	50.00	0		5.392	50.14	0.3	12.13
	100		3.442	100.0	0		2.700	100.1	0.1	17.15
	200		1.721	200.0	0		1.351	200.1	0.05	24.25

were tested. In addition, the moduli were identified through static tests (static loading of the plates). The displacements determined in the third cycle of loading, in both the dynamic deflectometer tests and the static tests, were considered to be reliable enough to be used for the computations (the first two cycles were regarded as trial loadings which stabilized the ground).

The vertical displacements of the ground base determined by means of the ZFG 02 deflectometer [5] were processed and the sought elasticity moduli  $\tilde{E}$  were determined using the proposed identification method. The obtained displacement diagrams are shown for selected kinds of ground base in Fig. 5. To verify the method, the determined values of  $\tilde{E}$  were compared with modulus values  $E_s$  identified by the conventional static method.

In the static load tests a pressure plate 0.3 m in diameter was used and the pressure of 0.1 MPa was applied (similarly as in the drop-weight tests). A diagram of the measurement is shown in



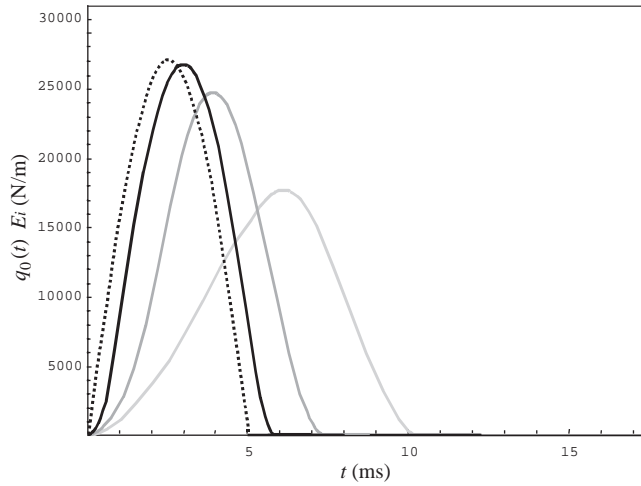


Fig. 4. Normalized graphs of displacement function  $q_0(t)E_i$  caused by an impulse of  $t_1 = 5$  ms duration for elasticity moduli:  $E_1 = 5$  MPa (—),  $E_2 = 25$  MPa (—),  $E_3 = 200$  MPa (—) and their quasi-static background (.....).

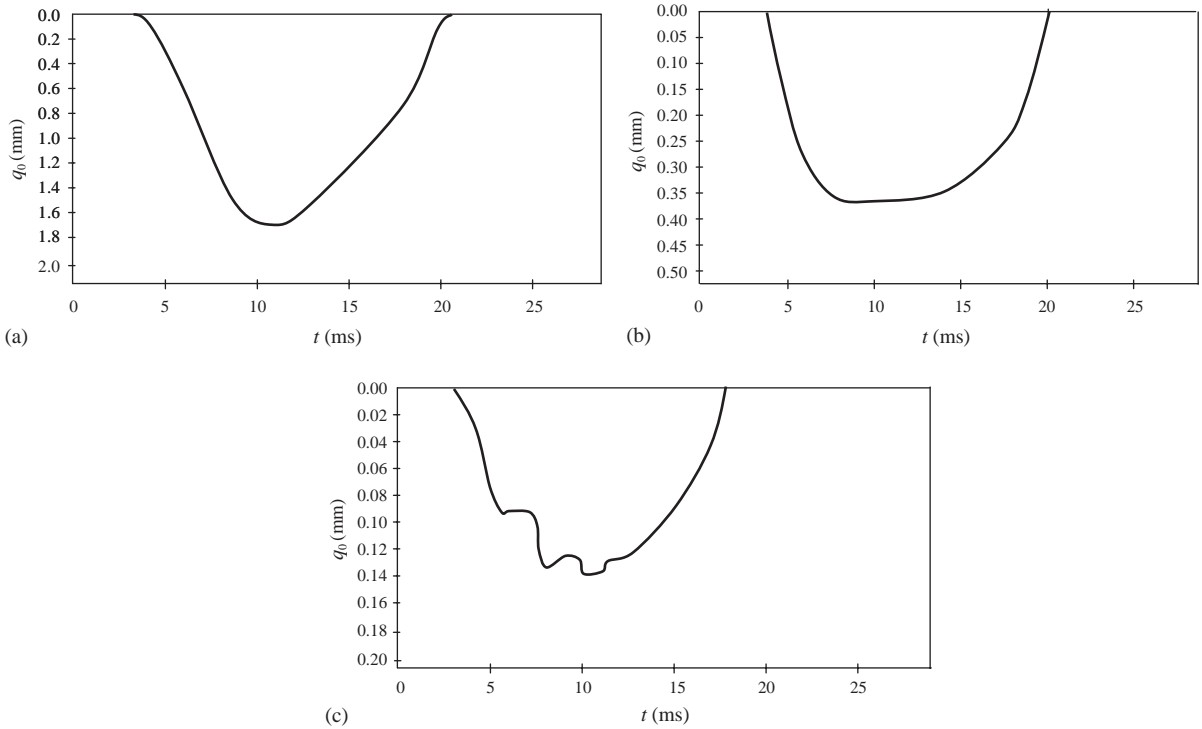


Fig. 5. Displacement diagrams obtained by means of Light Drop-Weight Tester ZFG02 for clay subsoil (a), sandy subsoil (b) and soil-cement base (c).

Fig. 6. The moduli were calculated from the classic formula (1). The static tests were performed as follows [2]. The plate was loaded up to 0.12 MPa in the first cycle of loading and up to 0.10 MPa in the 2nd and 3rd cycles. In each cycle, after the maximum load was reached, the load was lightened to zero. The difference between the displacement for 0.10 MPa in the 3rd cycle of loading and the displacement under the maximum load in this cycle is the calculation displacement (denoted as  $q_{s\max}$  in Fig. 6). This displacement was used to calculate the static moduli from relation (1).

The identified values of moduli  $\tilde{E}$  and  $E_s$  as well as the values of  $\tilde{E}$  determined from formula (14) are shown in Table 2. The tests were performed for the different consolidation indices. An analysis of the results shows that the modulus values identified by the proposed method are very similar to the static test results. The visible deviation for sand 4 may be due to the low consolidation index (0.90). If the results obtained from formula (9) are compared with the ones obtained from formula (14), it becomes apparent that in most cases the deviations are smaller for the proposed identification method.

### 7. Conclusions

The presented research has proved the viability of the proposed algorithm for identifying the moduli of elasticity of a ground base from the results of impact (drop-weight) tests. Since such tests take little time to perform, a large number of them can be carried out and thus a considerable

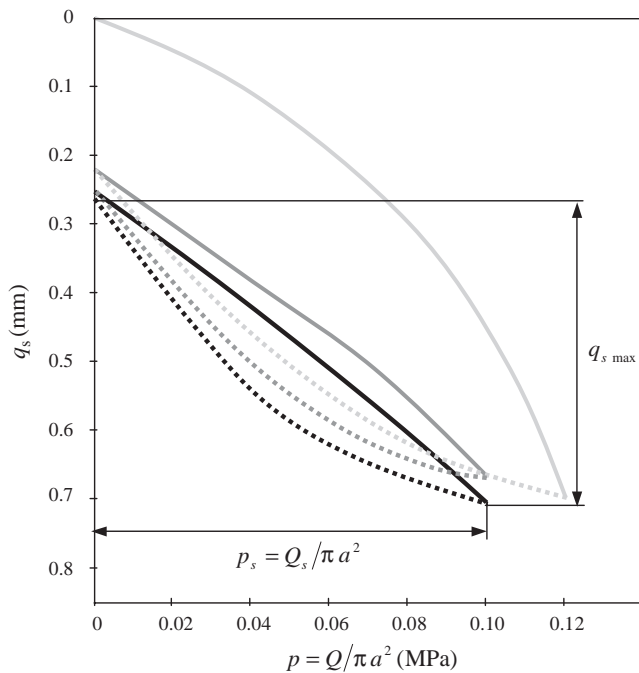


Fig. 6. Displacement versus load in static test: loading cycle I (—), loading cycle II (—), loading cycle III (—), unloading cycle I (.....), unloading cycle II (.....), unloading cycle III (.....).

Table 2  
Comparison of test results

No.	Subsoil type	Compaction index	Static test $E_s$ (MPa)	Proposed method $\tilde{E}$ (MPa)	Error $\frac{E_s - \tilde{E}}{E_s} 100\%$	Formula (14) $\tilde{E}$ (MPa)	Error $\frac{E_s - \tilde{E}}{E_s} 100\%$
1	Clay	0.99	16.8	17.19	2.3	16.07	4.3
2	Sand	0.98	66.3	62.37	5.9	75.65	14.1
3	Sand	0.94	39.2	36.47	7.0	45.46	16.0
4	Sand	0.90	31.3	25.65	18.1	33.26	6.3
5	10 cm thick soil-cement base on sand	—	230.0	220.19	4.3	190.18	17.3

area can be covered, which, considering the linear character of such structures as road and airfield pavements, is of no little importance. The following specific conclusions can be drawn:

1. The results shown in Table 1 prove that elasticity moduli  $\tilde{E}$  of a ground base can be accurately identified by the proposed method’s simulation test.
2. Tests carried out on actual ground bases showed the identified moduli of elasticity to be in agreement with the results obtained by the conventional static method.
3. Simplified formula (14) introduces errors (described in Section 5) whose magnitude depends on the velocity of propagation of transverse waves in the ground ( $c_2$ ) and the drop-weight tester’s parameters, i.e. impulse duration  $t_1$  and pressure plate radius  $a$ . The larger the errors, the lower is the ratio of impulse duration to the time which the Rayleigh wave needs to travel distance  $a$ . Thus the larger the errors, the shorter is the impulse duration and the higher are the values of the identified moduli of elasticity of the ground base.
4. The proposed identification method has no such drawbacks. The results it yields depend only on the actual values of the modulus of elasticity (for an assumed value of the Poisson ratio).

**Appendix A. Certain properties of solutions to linear equations of elastokinetics [6]**

Let surface load  $p(\mathbf{x}, t)$  with relative spatial distribution  $\phi(\mathbf{x})$  and resultant  $Q(t)$ , i.e.  $p(\mathbf{x}, t) = \phi(\mathbf{x})Q(t)$ , act on the boundary surface of a linearly viscoelastic body in time interval  $t \geq 0$ . As a result of this action, a vector displacement field, whose representation can be coordinate  $q_i(t)$  specifying the displacement of point “ $i$ ” in a certain direction, appears in the structure. Displacements  $q_i(t)$  can be expressed by the Duhamel integral. Assuming zero initial conditions  $q(0) = 0, \dot{q}(0) = 0$ , the integral has this form

$$q_i(t) = \int_0^t h_i(\tau)Q(t - \tau) d\tau, \tag{A.1}$$

where  $h_i(t)$  is the so-called impulse transition function, i.e. the response of point “ $i$ ” to a central unit impulse with spatial distribution  $\phi(r)$  and Dirac time distribution  $\delta(t)$ .

If a system is subjected to a surface load with spatial distribution  $\phi(\mathbf{x})$  and a resultant given by this formula

$$\hat{Q}(T) = \int_0^T Q(t) dt, \tag{A.2}$$

the displacement function is expressed by this formula

$$\hat{q}_i(T) = \int_0^T h_i(\tau) \hat{Q}(T - \tau) d\tau = \int_0^T h_i(\tau) \int_0^{T-\tau} Q(t) dt d\tau. \tag{A.3}$$

Using this relation

$$\int_0^{T-\tau} Q(t) dt = \int_\tau^T Q(t - \tau) dt \tag{A.4}$$

the following is obtained:

$$\hat{q}_i(T) = \int_0^T h_i(\tau) \int_0^{T-\tau} Q(t) dt d\tau = \int_0^T h_i(\tau) \int_\tau^T Q(t - \tau) dt d\tau = \int_0^T \int_\tau^T h_i(\tau) Q(t - \tau) dt d\tau. \tag{A.5}$$

The double integral on the right side of formula (A.5) is calculated over the area of the triangle shown in Fig. A.1. After the sequence of integration and the limits of integration in this integral are changed and relation (A.1) is applied, displacement function  $\hat{q}_i(t)$  finally assumes this form

$$\hat{q}_i(T) = \int_0^T \int_0^t h_i(\tau) Q(t - \tau) d\tau dt = \int_0^T q_i(t) dt. \tag{A.6}$$

Thus it has been proved (for the assumptions made) that if a load being an integral of  $Q(t)$ , i.e.  $\hat{Q}(t) = \int_0^t Q(t) dt$ , is introduced instead of load  $Q(t)$ , then instead of response  $q_i(t)$ , response  $\hat{q}_i(t)$  being an integral of  $q_i(t)$ , i.e.  $\hat{q}_i(t) = \int_0^t q_i(t) dt$ , will be obtained.

**Appendix B. Solution to elastic half-space vibration problem**

To determine the half-space displacements caused by any load uniformly distributed in circular area  $r \leq a$  (Fig. B.1) we shall use the solution to following well-known problem: if homogenous isotropic elastic half-space  $z \geq 0$  is loaded at edge  $z = 0$  with a concentrated normal force  $Q(t) =$

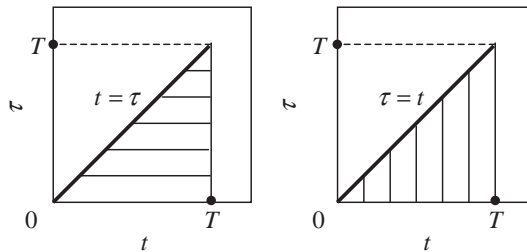


Fig. A.1. Integration range.

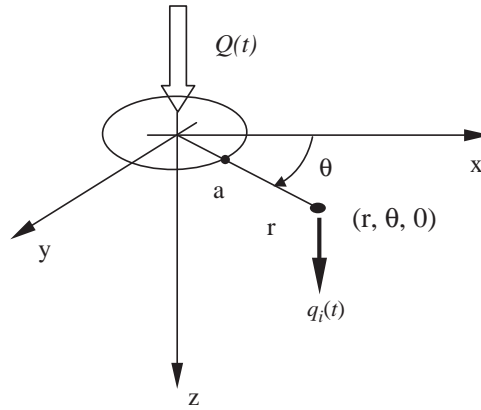


Fig. B.1. Diagram of system.

$QH(t)$ , where  $H(t)$  is the Heaviside function, then the function of vertical displacements  $w(r)$  at half-space edge  $z = 0$  is expressed by this formula

$$w(\tau) = w_1(\tau) = 0 \quad \text{for } 0 \leq \tau < \beta,$$

$$w(\tau) = w_2(\tau) = \frac{Q}{32\pi\mu(1-\beta^2)} \frac{1}{r} \left[ 4 + \frac{(\beta^2 - x_1^2)^{1/2}(1 - 2x_1^2)^2}{(x_3^2 - x_1^2)(x_1^2 - x_2^2)} (\tau^2 - x_1^2)^{-1/2} \right. \\ \left. + \frac{(\beta^2 - x_2^2)^{1/2}(1 - 2x_2^2)^2}{(x_1^2 - x_2^2)(x_2^2 - x_3^2)} (\tau^2 - x_2^2)^{-1/2} \right. \\ \left. + \frac{(x_3^2 - \beta^2)^{1/2}(1 - 2x_3^2)^2}{(x_2^2 - x_3^2)(x_3^2 - x_1^2)} (x_3^2 - \tau^2)^{-1/2} \right] \quad \text{for } \beta \leq \tau < 1,$$

$$w(\tau) = w_3(\tau)$$

$$= \frac{Q}{32\pi\mu(1-\beta^2)} \frac{1}{r} \left[ 8 + \frac{(x_3^2 - \beta^2)^{1/2} \left[ (1 - 2x_3^2)^2 + 4x_3^2(x_3^2 - \beta^2)^{1/2}(x_3^2 - 1)^{1/2} \right]}{(x_2^2 - x_3^2)(x_3^2 - x_1^2)} (x_3^2 - \tau^2)^{-1/2} \right]$$

for  $1 \leq \tau < x_3$ ,

$$w(\tau) = w_4(\tau) = \frac{Q}{4\pi\mu(1-\beta^2)} \frac{1}{r} \quad \text{for } x_3 \leq \tau, \tag{B.1}$$

where  $\tau = tc_2/r$ ,  $\beta = c_2/c_1 = \sqrt{(1-2\nu)/(2(1-\nu))}$ ;  $c_1 = \sqrt{(\lambda+2\mu)/\rho}$ ,  $c_2 = \sqrt{\mu/\rho}$  are the velocities of propagation of, respectively, longitudinal and transverse waves in the medium;  $\lambda$ ,  $\mu$  are Lamé constants and  $\rho$  is the medium's density. There are the following relationships between elasticity modulus  $E$  and the Poisson ratio  $\nu$ :  $\mu = E/(2(1+\nu))$ ,  $\lambda = E\nu/((1+\nu)(1-2\nu))$ . Parameters  $x_1$ ,  $x_2$ ,  $x_3$  in formula (B.1) are the roots of polynomial  $D(x)$

$$D(x) = 1 - 8x^2 + 8(3 - 2\beta^2)x^4 - 16(1 - \beta^2)x^6 \\ = -16(1 - \beta^2)(x^2 - x_1^2)(x^2 - x_2^2)(x^2 - x_3^2). \tag{B.2}$$

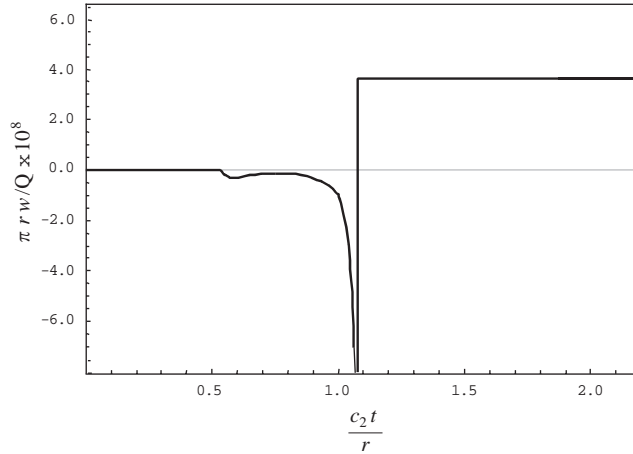


Fig. B.2. Function  $w(\tau)$  of half-space displacements caused by load  $H(t)\delta(r)/2\pi r$  for parameters  $E = 25$  MPa,  $\nu = 0.3$ ,  $\rho = 2000$  kg/m<sup>3</sup>.

The derivation of formula (B.1) can be found in Richard's paper [8]. A typical graph of displacement function  $w(\tau)$  for  $E = 25$  MPa,  $\nu = 0.3$ ,  $\rho = 2000$  kg/m<sup>3</sup> is shown in Fig. B.2, where symbols P, S and R denote moments at which the wavefront of, respectively, longitudinal wave P, transverse wave S and Rayleigh wave R reaches point  $(r, z) = (r, 0)$ . As one can see, displacements  $w(\tau)$  are equal to zero until longitudinal wave P reaches point  $(r, 0)$ . The reaching by transverse wave S of point  $(r, 0)$  manifests itself only by the discontinuity of the derivative of function  $w(\tau)$ .

When the load acting on the ground base has a uniform spatial distribution in a circle with radius  $a$  and its time distribution is still described by function  $H(t)$ , the displacement function for point  $(r, z) = (0, 0)$  is expressed by this formula

$$W(t) = W(r, t)|_{r=0} = \frac{2}{a^2} \int_0^a w(\tau)r \, dr = t^2 c_2^2 \int_{c_2 t/a}^{\infty} w(\tau) \frac{1}{\tau^3} \, d\tau, \quad (\text{B.3})$$

where  $\tau = tc_2/r$ . Since the form of function  $w(\tau)$  changes depending on the interval to which parameter  $\tau$  belongs, the form of function  $W(t)$  will change similarly:

$$W(t) = W_1(t) = \frac{2}{a^2} \left( \int_0^{c_2 t/x_3} w_4(\tau)r \, dr + \int_{c_2 t/x_3}^{c_2 t} w_3(\tau)r \, dr + \int_{c_2 t}^{c_2 t/\beta} w_2(\tau)r \, dr \right) \quad \text{for } 0 \leq t \frac{c_2}{a} < \beta,$$

$$W(t) = W_2(t) = \frac{2}{a^2} \left( \int_0^{c_2 t/x_3} w_4(\tau)r \, dr + \int_{c_2 t/x_3}^{c_2 t} w_3(\tau)r \, dr + \int_{c_2 t}^a w_2(\tau)r \, dr \right) \quad \text{for } \beta \leq t \frac{c_2}{a} < 1,$$

$$W(t) = W_3(t) = \frac{2}{a^2} \left( \int_0^{c_2 t/x_3} w_4(\tau)r \, dr + \int_{c_2 t/x_3}^a w_3(\tau)r \, dr \right) \quad \text{for } 1 \leq t \frac{c_2}{a} < x_3,$$

$$W(t) = W_4(t) = \frac{2}{a^2} \int_0^a w_4(\tau)r \, dr \quad \text{for } x_3 \leq t \frac{c_2}{a}, \quad (\text{B.4})$$

When formula (B.1) is taken into account and the integrations are calculated, the following is obtained

$$\begin{aligned}
 W(t) = W_1(t) = & \frac{c_2}{16\pi a^2 \mu (1 - \beta^2)} \left[ \left( 4 + \frac{4}{\beta} \right) t \right. \\
 & + \frac{(\beta^2 - x_1^2)^{1/2} (1 - 2x_1^2)^2 \left( \sqrt{1 - x_1^2} - \sqrt{1 - x_1^2/\beta^2} \right)}{x_1^3 (x_3^2 - x_1^2) (x_1^2 - x_2^2)} t \\
 & + \frac{(\beta^2 - x_2^2)^{1/2} (1 - 2x_2^2)^2 \left( \sqrt{1 - x_2^2} - \sqrt{1 - x_2^2/\beta^2} \right)}{x_2^3 (x_1^2 - x_2^2) (x_2^2 - x_3^2)} t \\
 & - \frac{(x_3^2 - \beta^2)^{1/2} (1 - 2x_3^2)^2 \left( \sqrt{x_3^2 - 1} - \sqrt{x_3^2/\beta^2 - 1} \right)}{x_3^3 (x_2^2 - x_3^2) (x_3^2 - x_1^2)} t \\
 & \left. + \frac{(x_3^2 - \beta^2)^{1/2} \sqrt{x_3^2 - 1} \left( (1 - 2x_3^2)^2 + 4x_3^2 (x_3^2 - \beta^2)^{1/2} (x_3^2 - 1)^{1/2} \right)}{x_3^3 (x_2^2 - x_3^2) (x_3^2 - x_1^2)} t \right] \\
 \text{for } 0 \leq t \frac{c_2}{a} < \beta, & \tag{B.5)_1}
 \end{aligned}$$

$$\begin{aligned}
 W(t) = W_2(t) = & \frac{c_2}{16\pi a^2 \mu (1 - \beta^2)} \left[ \left( \frac{4a}{c_2} + 4t \right) \right. \\
 & - \frac{(\beta^2 - x_1^2)^{1/2} (1 - 2x_1^2)^2 \left( \sqrt{t^2 - x_1^2 a^2 / c_2^2} - \sqrt{1 - x_1^2 t} \right)}{x_1^3 (x_3^2 - x_1^2) (x_1^2 - x_2^2)} \\
 & - \frac{(\beta^2 - x_2^2)^{1/2} (1 - 2x_2^2)^2 \left( \sqrt{t^2 - x_2^2 a^2 / c_2^2} - \sqrt{1 - x_2^2 t} \right)}{x_2^3 (x_1^2 - x_2^2) (x_2^2 - x_3^2)} \\
 & + \frac{(x_3^2 - \beta^2)^{1/2} (1 - 2x_3^2)^2 \left( \sqrt{x_3^2 a^2 / c_2^2 - t^2} - \sqrt{x_3^2 / \beta^2 - 1 t} \right)}{x_3^3 (x_2^2 - x_3^2) (x_3^2 - x_1^2)} \\
 & \left. + \frac{(x_3^2 - \beta^2)^{1/2} \sqrt{x_3^2 - 1} \left( (1 - 2x_3^2)^2 + 4x_3^2 (x_3^2 - \beta^2)^{1/2} (x_3^2 - 1)^{1/2} \right)}{x_3^3 (x_2^2 - x_3^2) (x_3^2 - x_1^2)} t \right] \\
 \text{for } \beta \leq t \frac{c_2}{a} < 1, & \tag{B.5)_2}
 \end{aligned}$$

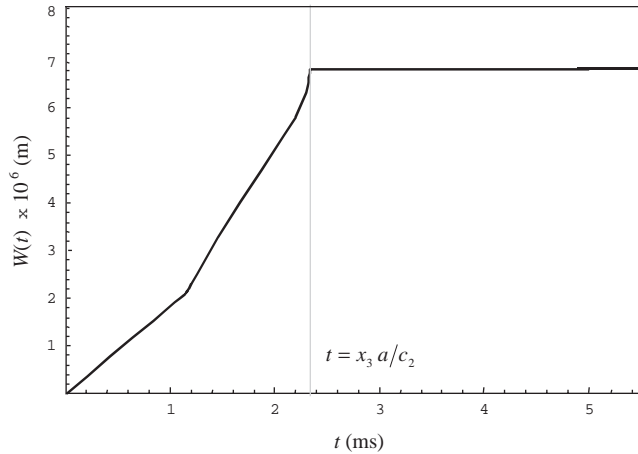


Fig. B.3. Function  $W(t)$  of half space displacements caused by load  $H(t)$  for parameters  $E = 25 \text{ MPa}$ ,  $\nu = 0.3$ ,  $\rho = 2000 \text{ kg/m}^3$ .

$$W(t) = W_3(t) = \frac{c_2}{16\pi a^2 \mu (1 - \beta^2)} \left[ \frac{8a}{c_2} + \frac{(x_3^2 - \beta^2)^{1/2} \sqrt{x_3^2 a^2 / c_2^2 - t^2} \left( (1 - 2x_3^2)^2 + 4x_3^2 (x_3^2 - \beta^2)^{1/2} (x_3^2 - 1)^{1/2} \right)}{x_3^3 (x_2^2 - x_3^2) (x_3^2 - x_1^2)} \right] \quad \text{for } 1 \leq t \frac{c_2}{a} < x_3, \tag{B.5}_3$$

$$W(t) = W_4(t) = \frac{1}{2\pi \mu a (1 - \beta^2)} \quad \text{for } x_3 \leq t \frac{c_2}{a}. \tag{B.5}_4$$

An exemplary graph of displacement function  $W(t)$  for  $E = 25 \text{ MPa}$ ,  $\nu = 0.3$ ,  $\rho = 2000 \text{ kg/m}^3$  is shown in Fig. B.3. Displacements  $W(t)$  assume a constant value until the moment when the Rayleigh waves generated at the boundary of the area in which the load acts (in the considered case the boundary is a circle  $r = a$ ) reach central point  $(0, 0)$ . The time in which the Rayleigh waves cover this distance is  $t = x_3 a / c_2$ .

To obtain the vertical displacement of point  $(r, z) = (0, 0)$  for any time distribution of load function  $Q(t)$  one should calculate this integral

$$q_0(t) = Q(0_+)W(t) + \int_0^t \frac{dQ(\tau)}{d\tau} \cdot W(t - \tau) d\tau. \tag{B.6}$$

In the case of loads of finite duration ( $t_1 < \infty$ ), system response duration  $q_0(t)$  is also finite and it amounts to  $T_a = t_1 + x_3 a / c_2$ . This can be shown by integrating convolution (B.6) by parts and exploiting the fact that  $W(0) = 0$ .



## References

- [1] D. Croney, P. Croney, *Design and Performance of Road Pavements*, McGraw-Hill, New York, 1998.
- [2] R. Floss, *Zusätzliche Technische Vertragsbedingungen und Richtlinien für Erdarbeiten im Strassenbau, Kommentar mit Kompendium Erd- und Felsbau*, Kirschbaum Verlag, Bonn, 1997.
- [3] M.J.H. Stet, M.E. van de Bol-de Jong, J.P. Verbeek, *Dutch standard for evaluation of concrete airfield pavements, Proceedings Federal Aviation Administration, Technology Transfer Conference*, Atlantic City, NJ, USA, 1999.
- [4] P. Ullidtz, *Pavement Analysis*, Elsevier, Amsterdam, 1987.
- [5] Light Drop-Weight Tester ZFG02. *Operating Manual*. Zorn Stendal, Germany, 1996.
- [6] J. Langer, P. Ruta, Dynamic identification of model parameters of road and airfield pavements, *Archives of Civil Engineering* 41 (2) (1995) 115–136.
- [7] D. Cebon, *Handbook of Vehicle–Road Interaction*, Swets & Zeitlinger B.V., Lisse, The Netherlands, 1999.
- [8] P.G. Richards, Elementary solutions to Lamb’s problem for a point source and their relevance to three-dimensional studies of spontaneous crack propagation, *Bulletin of the Seismological Society of America* 69 (4) (1979) 947–956.